Responsiveness of G protein-coupled odorant receptors is partially attributed to the activation mechanism

Yiqun Yu[a,1], Claire A. de March[b,1], Mengjue J. Ni[c], Kaylin A. Adipietro[c], Jérôme Golebiowski[b,2], Hiroaki Matsunami[c,d,e,2], and Minghong Ma[a,2]

[a]Department of Neuroscience, University of Pennsylvania Perelman School of Medicine, Philadelphia, PA 19104; [b]Institute of Chemistry Nice, UMR 7272, University Nice Sophia Antipolis, Centre National de la Recherche Scientifique, 06108 Nice Cedex 2, France; [c]Department of Molecular Genetics and Microbiology, Duke University Medical Center, Durham, NC 27710; [d]Department of Neurobiology, Duke University Medical Center, Durham, NC 27710; and [e]Duke Institute for Brain Sciences, Duke University Medical Center, Durham, NC 27710

Edited by Jeremy W. Thorner, University of California, Berkeley, CA, and approved October 23, 2015 (received for review September 2, 2015)

Mammals detect and discriminate numerous odors via a large family of G protein-coupled odorant receptors (ORs). However, little is known about the molecular and structural basis underlying OR response properties. Using site-directed mutagenesis and computational modeling, we studied ORs sharing high sequence homology but with different response properties. When tested in heterologous cells by diverse odorants, MOR256-3 responded broadly to many odorants, whereas MOR256-8 responded weakly to a few odorants. Out of 36 mutant MOR256-3 ORs, the majority altered the responses to different odorants in a similar manner and the overall response of an OR was positively correlated with its basal activity, an indication of ligand-independent receptor activation. Strikingly, a single mutation in MOR256-8 was sufficient to confer both high basal activity and broad responsiveness to this receptor. These results suggest that broad responsiveness of an OR is at least partially attributed to its activation likelihood.

G protein-coupled receptor | odorant receptor | broad responsiveness | site-directed mutagenesis | computational modeling

G protein-coupled receptors (GPCRs) are seven transmembrane (TM) proteins which play essential roles in converting extracellular stimuli into intracellular signals in a variety of cell types. Odor detection by olfactory sensory neurons (OSNs) in the mammalian nose depends on a large family of G protein-coupled odorant receptors (ORs) (1), which endows the olfactory system with an extraordinary power of odor detection and discrimination. Although OR-ligand binding is the first step toward smell perception, little is known about the molecular and structural basis underlying odor response properties of individual ORs.

Most mammalian ORs respond to a small fraction of all of the tested odorants (2). In contrast, recent studies have identified a small number of ORs that respond to a large set of diverse odorants with comparable potency and efficacy as the former. Curiously, several broadly responsive ORs including MOR256-3 (Olfr124 or SR1), MOR256-31 (Olfr263), and human OR2W1 (ortholog of MOR256-31) belong to the same subfamily, which also contains ORs such as MOR256-8 (Olfr1362) and MOR256-22 (Olfr1387) that respond to a few odorants (3–6). Identification of ORs within the same subfamily (i.e., sharing >50% amino acid identity) but with different response properties offers an opportunity for dissecting out the molecular features that define the tuning properties of these ORs.

Mammalian ORs belong to class A (or *rhodopsin* family) GPCRs. The structure-function relationship of several class A members (e.g., rhodopsin and β2-adrenergic receptor) has been investigated in great details via various approaches including site-directed mutagenesis, X-ray crystallography (7, 8), and molecular modeling (9–11). Although no crystal structure is available for any OR, site-directed mutagenesis and/or computational modeling have shed light on structure-function relationship for a few ORs (12–18).

Using a joint approach of site-directed mutagenesis and computational modeling, we investigated the response properties of mutant ORs based on MOR256-3 and MOR256-8, which responded to a large and small set of odorants, respectively. Three-dimensional atomic models of these ORs were built to map locations of the mutated residues. Most mutations in MOR256-3 altered the responses to different odorants in a similar manner. Remarkably, MOR256-8 was converted into a broadly responsive OR by swapping a single or a few residues. More generally, we found that an OR's total response was positively correlated with its basal activity, an indication of ligand-independent receptor activation. These data suggest that broad responsiveness of an OR is not only determined by ligand binding, but also by activation mechanism.

Results

Identification of Residues That Potentially Underlie Broad Responsiveness of MOR256-3. Ideally, the response profile of an OR should be determined based on an exhaustive list of odorants, which would be time consuming if not impossible given the almost infinite odor space. To provide a numerical description of broadly responsive ORs, we analyzed the percentage of odorants a receptor responds to from an array of 62 ORs from different subfamilies vs. 63 diverse odorants reported in a previous study (5). The median was 4.8%, and the median absolute deviation (MAD) was 7.0%, indicating that any OR responding to 25.8% of the odorants would be 3 MAD away from the median. We hence defined an OR as broadly responsive if

Significance

Mammalian odorant receptors (ORs) comprise the largest family of G protein-coupled receptors, which are frequent drug targets. While many ORs respond specifically to select odorants, recent studies have identified a small number of ORs that respond to a large set of diverse odorants. Up to date, little is known about the molecular and structural features that shape the OR response properties. Our study reveals that broadly responsive ORs show elevated basal activity, suggesting a lower activation barrier. Surprisingly, a single amino acid mutation is sufficient to confer high basal activity and broad responsiveness to an OR, which originally shows weak responses to few odorants.

Author contributions: Y.Y., C.A.d.M., J.G., H.M., and M.M. designed research; Y.Y., C.A.d.M., M.J.N., and K.A.A. performed research; Y.Y., C.A.d.M., M.J.N., K.A.A., J.G., H.M., and M.M. analyzed data; and Y.Y., C.A.d.M., J.G., H.M., and M.M. wrote the paper.

The authors declare no conflict of interest.

This article is a PNAS Direct Submission.

[1]Y.Y. and C.A.d.M. contributed equally to this work.

[2]To whom correspondence may be addressed. Email: minghong@mail.med.upenn.edu, matsu004@mc.duke.edu, or jerome.golebiowski@unice.fr.

This article contains supporting information online at www.pnas.org/lookup/suppl/doi:10.1073/pnas.1517510112/-/DCSupplemental.

it responds to ≥30% (a more stringent criterion rounded from 25.8%) of a given set of diverse odorants, which covers a significant portion of the odor space (19). This definition offers an appropriate description of ORs with exceptionally broad response profiles using different sets of odorants (Fig. S1). To minimize the effects of odorant concentrations on the OR response profiles, all ORs were tested at the same concentrations and a positive response was determined at 300 μM, a near-saturating concentration.

We initially focused on the broadly responsive MOR256-3 receptor, which was extensively studied both in genetically tagged OSNs and in a heterologous expression system (3). We compared the response properties of the following five ORs within the same family. Out of 22 diverse odorants tested, MOR256-3, MOR256-31, and hOR2W1 exhibited broad responsiveness. In contrast, MOR256-8 and MOR256-22 responded weakly to a few odorants (Fig. 1*A*). Their response profiles were further assessed by dose–response analysis on selected odorants or a larger odorant set (Fig. S1 and ref. 5). Note that odorant-induced responses are not correlated with the receptor surface expression levels (see below).

To identify key residues that underlie broad responsiveness, we aligned the protein sequences of these five ORs from the same subfamily (Fig. 1*B* and Fig. S2) and built 3D atomic models of MOR256-3 and MOR256-8 (Fig. 2*A*) (18, 20). We constructed 36 site-directed mutant MOR256-3 ORs mostly by substituting the residues conserved in the broadly responsive ORs to those in MOR256-8 or MOR256-22 individually or in combination. The mutated sites included all 17 conserved residues between TM3 and TM6 plus six located in TM1 and TM2 (Figs. 1*B* and 2*A*).

All MOR256-3 mutants except T161P are expressed at the cell surface (Fig. S3) and differentially influence odorant-induced responses (Figs. 2 and 3 and Table S1). Eighteen mutations significantly decreased, 7 significantly increased, and 10 did not change the overall responses (Figs. 2*B* and 3 *A*–*D*). Notably, switching a single residue in TM3 of MOR256-3 to that of MOR256-8 (denoted as 3 Y102F or 3 L107I) drastically decreased the odor responses by >70% (Figs. 2*B* and 3 *A* and *B*). When the responses to individual odorants at 300 μM were ranked, most mutant ORs showed the same ranking order as wild-type (WT) MOR256–3 [from the strongest to weakest ligand: 1-octanol, (−) carvone, coumarin, benzyl acetate, and allyl phenyl acetate] with a few exceptions (e.g., G108A, L199M, G203A, and T254S) (Figs. 3 *A*–*D* and 4*A*), suggesting that most of the mutated residues are not governing binding to specific odorants but rather affecting the overall responsiveness.

Curiously, ORs with strong odorant responses tended to show higher basal activities (Fig. 4*A*). Regression analysis on the data set including the five WT ORs and all 35 functional mutant MOR256-3 ORs confirmed that the total response of an OR was positively correlated with the basal activity (Fig. 4*B*). In contrast, neither the total response nor the basal activity was correlated with the OR surface expression level (Fig. 4*C*). These data support that more responsive ORs have a higher basal activity level, implying a higher probability of receptor activation.

A Single Mutation Confers Broad Responsiveness to MOR256-8. MOR256-8 shares more than 50% amino acid identity with other broadly responsive members in the same subfamily. Because in MOR256-3, substituting single residues by those in MOR256-8 led to complete loss of surface expression (3 T161P) or significantly reduced odorant responses (3 Y102F and 3 L107I) (Figs. 2–4 and Fig. S3), we asked whether reversely swapping these residues would confer broad responsiveness to MOR256-8. All mutant MOR256-8 ORs described below showed surface expression and their responses were not correlated with the expression levels (Fig. 5*C*). Single mutations 8 F102Y and 8 P161T responded to three and six odorants, respectively, more than WT MOR256-8, which responded to 2 of the 22 odorants. Strikingly, mutations 8 I107L and 8 I107L P161T responded to 45.5% and 40.9% of the odorant set, respectively, indicating that they are broadly responsive (Fig. 5*A*). Triple mutation 8 F102Y I107L P161T did not respond more

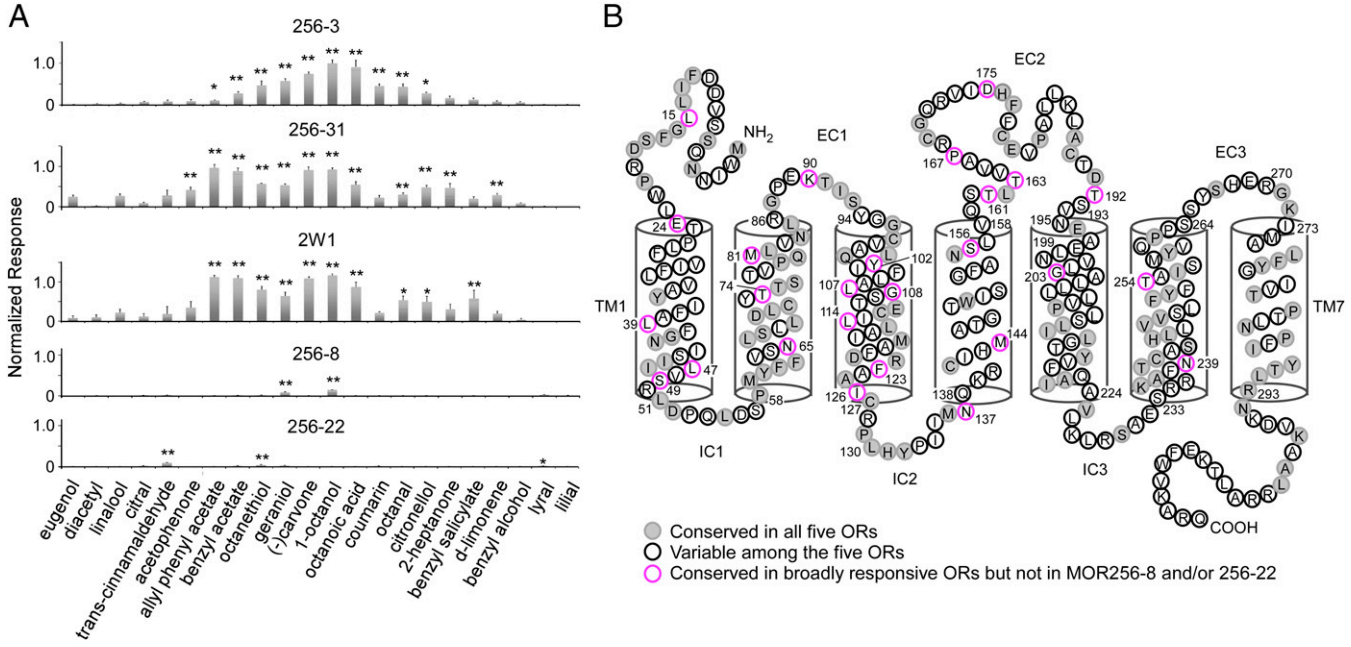

Fig. 1. The MOR256 subfamily contains ORs with different response properties. (*A*) Responses of different ORs to a set of 22 odorants (all at 300 μM) in Hana3A cells (mean ± SEM). All odorant-OR pairs were tested on at least two plates (with three repeats on each plate). A positive response was identified if it was significantly higher than the basal activity (*$P < 0.05$ and **$P < 0.01$ in one-way ANOVA post hoc Dunnett's tests). MOR256-3, MOR256-31, and 2W1 responded to 10, 12, and 10 compounds (or 45.5%, 54.5%, and 45.5%), respectively. MOR256-8 and MOR256-22 showed weak but significant responses to two and three odorants, respectively, due to their low basal activity. All responses were normalized to WT MOR256-3's response to 1-octanol at 300 μM and corrected for surface expression (see *Materials and Methods* for details). (*B*) Snake plot of the MOR256-3 receptor, which contains 315 amino acids with 114 conserved in all five ORs (filled in gray). The transmembrane domains are determined by the 3D atomic model (see also Fig. 2*A*). Magenta circles mark residues that are conserved in the three broadly responsive ORs (MOR256-3, MOR256-31, and 2W1), but not in MOR256-8 and/or MOR256-22.

A

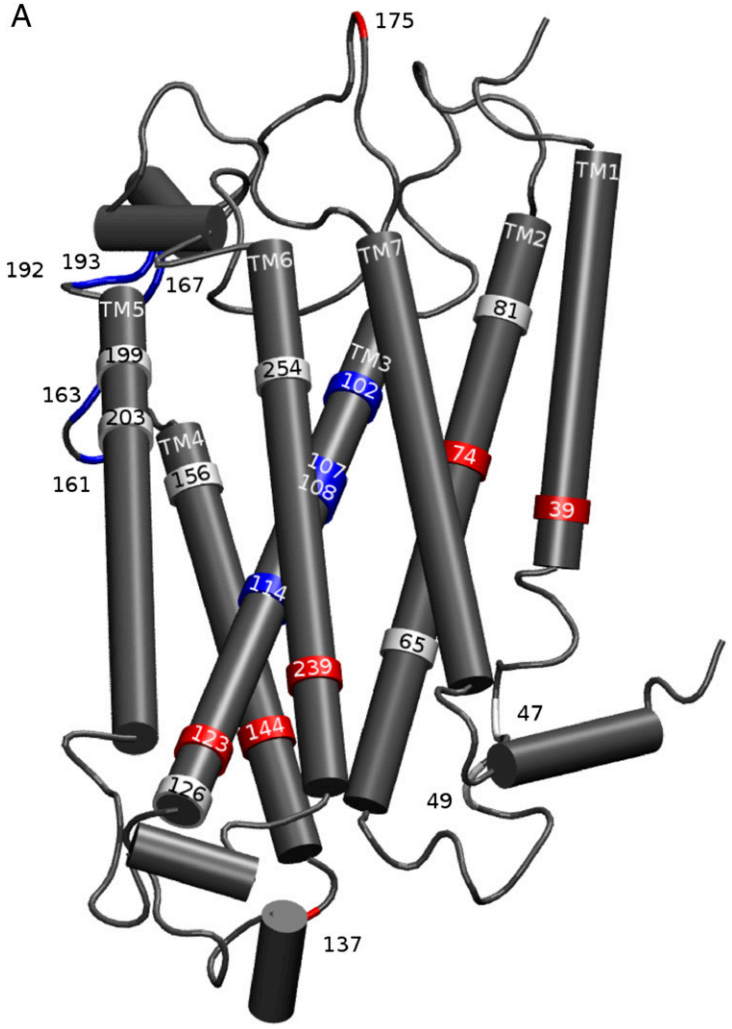

B

Domain	MOR256-3 ORs	Total Response	*p* Value
	WT	1.00	
TM1	**L39V**	1.98	**
	L47V	0.91	ns
	S49C	0.94	ns
TM2	N65H	1.02	ns
	T74S	1.69	**
	M81L	1.02	ns
TM3	**Y102F**	0.22	**
	Y102F G108A L114I	0.16	**
	L107I	0.26	**
	G108A	0.44	*
	L114I	0.81	*
	F123Y	1.33	**
	I126V	0.89	ns
IC2	**N137H**	2.25	**
TM4	**M144L**	1.28	*
	S156A	1.04	ns
EC2	T161A	0.49	**
	T161C	0.55	**
	T161G	0.50	**
	T161G T163V	0.18	**
	T161P	no expression	
	T161P T163A	0.39	*
	T161S	0.97	ns
	T161V	0.57	**
	T163A	0.71	**
	T163P	0.11	**
	T163V	0.55	**
	P167R	0.59	*
	D175N	1.39	**
	T192A	0.52	*
	T192P	0.23	**
	S193R	0.58	**
TM5	L199M	0.84	ns
	G203A	1.01	ns
TM6	N239G	1.93	**
	T254S	0.94	ns

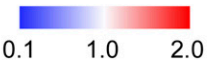

Fig. 2. Summary of the total response of mutant MOR256-3 ORs. (*A*) Mutated residues are shown in the 3D atomic model of MOR256-3. Red, blue, and gray colors indicate increased, decreased, and unchanged total response (see below), respectively. The MOR256-8 model looks identical to MOR256-3 regarding the position of each residue. (*B*) The total response is the sum of the responses to all five odorants at 300 μM, normalized to that of WT MOR256-3 tested on the same plate and corrected for surface expression. EC, extracellular loop; IC, intracellular loop; TM, transmembrane domain. The mutants in bold mark residue swaps between MOR256-3 and MOR256-8. One-way ANOVA post hoc Dunnett's tests were performed for each mutant and WT pair (ns = not significantly different, $*P < 0.05$, and $**P < 0.01$). The responses to individual odorants are reported in Fig. 4*A* and Table S1.

broadly than 8 I107 and 8 I107L P161T (Fig. 5*A*), suggesting that the effects of these residues are not additive. Compared with WT MOR256-8, the broadly responsive mutant ORs showed higher basal activity (Fig. 5*B*) as other broadly responsive ORs (Fig. 4).

Discussion

In the current study, we investigated the molecular and structural features underlying the broad responsiveness of MOR256-3 using site-directed mutagenesis and computational modeling. We identified a handful of residues in MOR256-3 that are critical for its response properties (Figs. 1–3). We further demonstrate that the basal activity of an OR is strongly correlated with its overall responsiveness (Fig. 4). Remarkably, MOR256-8, which weakly responds to a few odorants, can be converted into a broadly responsive receptor by mutation of a single or a few residues (Fig. 5). These data provide unprecedented insights into the mechanisms underlying the response properties of mammalian ORs and GPCRs in general.

Our study suggests that the activation mechanism of an OR significantly impacts its response properties. The major difference between MOR256-3 and MOR256-8 likely resides in the receptor activation process. Many single mutations in MOR256-3 alter its response efficacy and potency to all odorants in a similar manner (Figs. 2–4). Strikingly, mutation of a single (at position 107) or a few residues in MOR256-8 confers both high basal activity and broad responsiveness to this receptor. Interestingly, residue 107 is at the vicinity of G108 (identical between MOR256-3 and MOR256-8) and mutation G108L in MOR256-3 leads to a constitutively active receptor (18). This position is located at the crossing of TM3 and TM6 and is reported to form a cradle for the ligand in class A GPCRs (21). It is plausible that mutation at 107 and many other residues examined in this study change the likelihood of receptor activation rather than binding to specific ligands.

A broadly responsive OR (such as MOR256-3) would require a low activation barrier in addition to a permissive binding pocket. Unlike most nonolfactory GPCRs, which use ionic or hydrogen bond interactions to ensure selectivity and sensitivity in binding their agonists or antagonists (22), ORs bind to their ligands via much weaker van der Waals interactions (14, 16, 23). It is conceivable that at least some ORs have a permissive binding

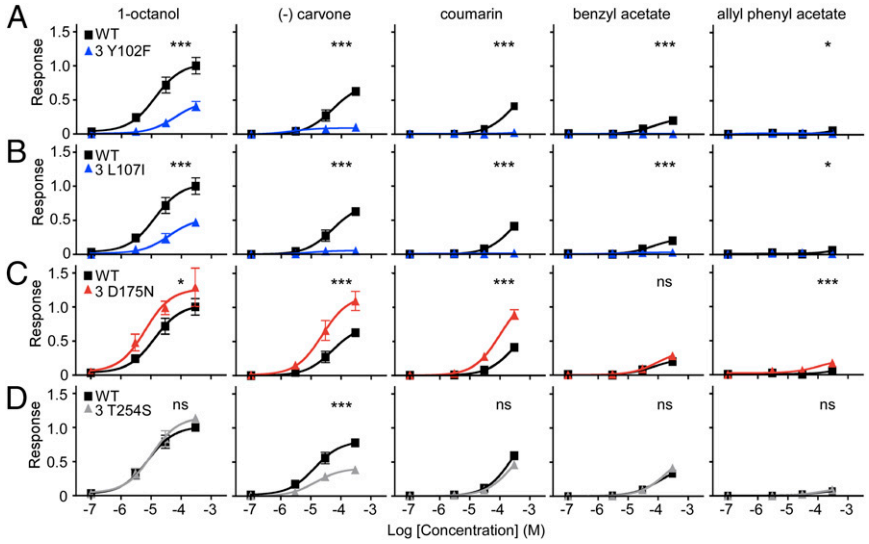

Fig. 3. Mutations at different residues differentially change the response properties of MOR256-3. (*A* and *B*) Single mutations 3 Y102F (*A*) and 3 L107I (*B*) decreased the responses to all five odorants. (*C*) A single mutation 3 D175N increased the responses to four out of five odorants. (*D*) A single mutation 3 T254S selectively reduced the response to (–) carvone. Each mutant OR was tested on the same plate as WT (three repeats for each OR; mean ± SEM) and all responses were normalized to WT response to 1-octanol at 300 μM and corrected for surface expression. Two-way ANOVA (concentration and OR type) tests were performed for each mutant and WT pair (ns = not significantly different, $*P < 0.05$, $**P < 0.01$, and $***P < 0.001$ for OR type).

cavity where the interaction would be more opportunistic compared with other GPCRs (14). Therefore, binding of many distinct ligands can lead to receptor activation.

On the other hand, an OR that appears as "selectively responsive" could result from two scenarios: either this OR has a truly restrictive binding cavity or it has a high activation barrier for activation. We suspect that MOR256-8 belongs to the latter because mutation of a single or a few residues can convert it into a broadly responsive OR (Fig. 5).

The positive correlation between broad responsiveness and basal activity described here (Figs. 4 and 5) does not imply that the basal activity alone is sufficient to predict the response properties of a given OR. This correlation may only apply to some ORs and operate within a certain range. For example, a constitutively active mutant OR (with extremely high basal activity) can lose its capability of responding to odorants (18). Many residues in addition to the ones investigated here may also contribute to an OR's response properties by affecting ligand binding and/or receptor activation.

Broadly responsive ORs are identified from insects to humans (5, 24), and the selective advantages of these ORs in smell perception may be multifaceted. First, these receptors can potentially increase the range of detectable odors for the olfactory system. Second, they may contribute to an organism's ability in odor discrimination via the combinatorial scheme. In the retina, three types of cones with broad tuning spectra are sufficient for color perception. Third, these receptors may serve as general odor detectors. Curiously, OSNs expressing MOR256-3 are highly concentrated in the septal organ, a chemosensory organ located in the ventral base of the nasal septum and in the direct air path (25). The broadly responsive OSNs in the septal organ and the main olfactory epithelium may inform the system the presence of any odor in the environment. Fourth, these receptors may act as intensity analyzers by providing the olfactory system an easier readout on odor concentrations regardless of the identity of the odors.

Materials and Methods

Site-Directed Mutagenesis. The coding sequences of MOR256 receptors were amplified from genomic DNA of C57BL/6 mice and subcloned into the pcDNA3.1/TOPO vector (Invitrogen) with an N-terminal tag of the first 20 amino acids of rhodopsin (Rho). Site-directed mutants were constructed using the Quikchange site-directed mutagenesis kit (Agilent Technologies). The sequences of all plasmid constructions were verified by both forward and reverse sequencing (DNA sequencing core facility, University of Pennsylvania).

Luciferase Assay in Hana3A Cells. The Dual-Glo Luciferase Assay (Promega) was used to determine the activities of firefly and Renilla luciferase in Hana3A cells (26). Firefly luciferase, driven by a cAMP response element promoter (CRE-Luc; Stratagene), was used to determine OR activation levels. Renilla luciferase, driven by a constitutively active SV40 promoter (pRLSV40; Promega), functioned as an internal control for transfection efficiency and cell viability. Hana3A cells, a HEK293T-derived cell line stably expressing the receptor-transporting proteins (RTP1L and RTP2), receptor expression-enhancing protein 1 (REEP1), and olfactory G protein ($G_{\alpha olf}$) (26), were plated on poly-D-lysine-coated 96-well plates (Nalge Nunc) and incubated overnight in minimum essential medium eagle (Sigma) with 10% FBS at 37 °C and 5% CO_2. The following day, cells were transfected using Lipofectamine 2000 (Invitrogen). For each 96-well plate, 0.5 μg of pRL-SV40, 1 μg of CRE-Luc, 0.5 μg of mouse RTP1S, 0.25 μg of mouse muscarinic acetylcholine receptor M3 and 0.5 μg of receptor plasmid DNA were transfected. After transfection (24 h), medium was replaced with 25 μL of odorant solution diluted in CD293 chemically defined medium (Invitrogen), and cells were further incubated for 4 h at 37 °C and 5% CO_2. The manufacturer's protocols were followed to measure firefly luciferase and Renilla luciferase activities. Raw data were analyzed according to the published procedure using Microsoft Excel and GraphPad Prism (26).

To facilitate comparison between OR responses from multiple plates, we always included Rho-tag empty vector and WT MOR256-3 as negative and positive control, respectively. The basal activity of an OR was averaged from four wells in the absence of odorants. An odorant-induced response was obtained by subtracting the basal activity of that receptor. In experiments where the five odorants [1-octanol, (–) carvone, coumarin, benzyl acetate, and allyl phenyl acetate] were tested, the responses to each odorant at four concentrations (0, 3, 30, and 300 μM) were measured. The sum of the responses to all five odorants at 300 μM was used to evaluate an OR's overall responsiveness. All odorant responses and basal activities were normalized to MOR256-3's response to 300 μM 1-octanol.

Evaluation of OR Surface Expression and Data Correction. Live-cell immunostaining was used to evaluate OR surface expression (26). Hana3A cells were cotransfected with receptor and GFP plasmids 24 h before the staining. The transfected Hana3A cells were incubated with primary antibody solution (mouse anti-rhodopsin, Rho 4D2, Abcam) on ice for 1 h. After rinsing the cells three times, secondary antibody solution (Alexa Fluor 568-conjucated anti-mouse IgG) was added onto the cells, and incubated for 45 min on ice. At the end of the

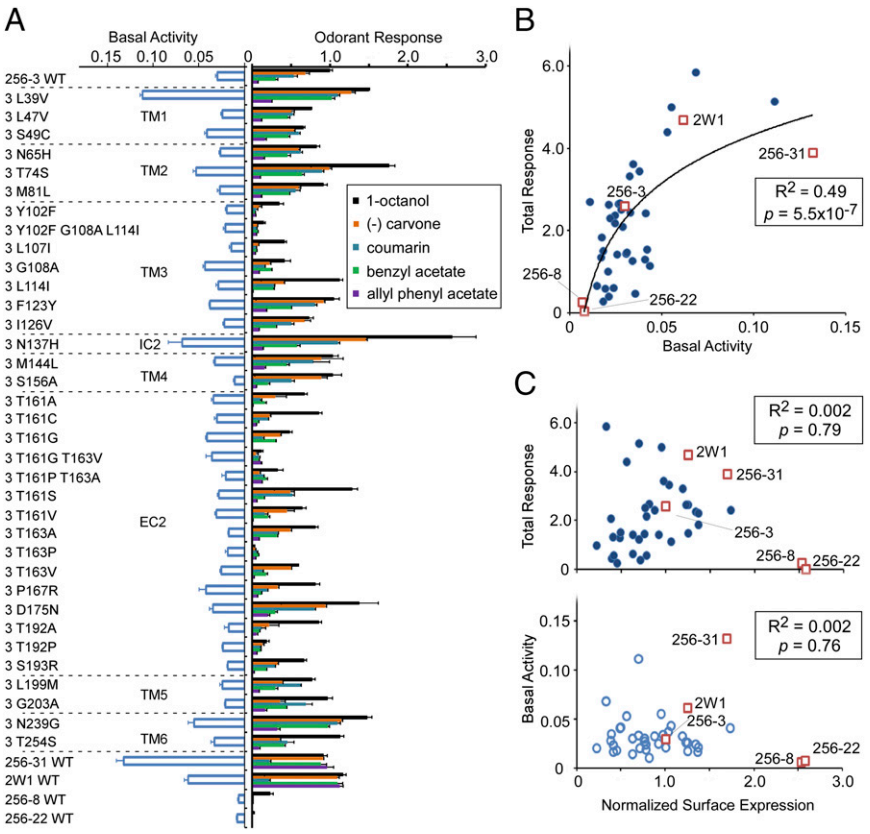

Fig. 4. The total response of an OR is positively correlated with its basal activity. (*A*) Summary of the basal activity (*Left*) and the responses to all five odorants at 300 μM (*Right*) for each OR. The five odorants were ranked based on the responses of WT MOR256-3 from largest to smallest. The odorant responses for each OR were averaged from three repeats on the same plate except for WT ORs, averaged from 8 to 21 plates (mean ± SEM). The basal activity for each OR was averaged from four repeats on the same plate. All odorant responses and basal activities were normalized to WT MOR256-3's response to 1-octanol at 300 μM and corrected for surface expression. (*B*) The total response to all five odorants at 300 μM was plotted against its basal activity for each OR. The curved line represents logarithmic regression fitting because it models the fact that the odorant-induced response did not rise linearly but instead reached a plateau even for an extremely broadly responsive OR. (*C*) Neither the total response nor the basal activity of WT and mutant ORs was correlated with the receptor surface expression (see Fig. S3 for the surface expression of each OR) via linear regression analysis.

incubation, the cells were fixed with 2% (wt/vol) paraformaldehyde, and mounted with vectashield mounting medium (Vector Laboratories).

The surface expression of each OR was quantified by the Rho/GFP intensity ratio, which takes into account both the number of transfected cells and the expression level in individual cells. For each plate, the total fluorescence intensity (after background subtraction) was measured for both red (Rho) and green (GFP) channels using Image J. The intensity ratio (Rho/GFP) was obtained for all WT and mutant ORs (Fig. S3). All odorant responses and basal activities were corrected for OR surface expression by dividing the Rho/GFP intensity ratio scaled to WT MOR256-3.

For selected ORs (Fig. S3), the surface expression was also evaluated using fluorescence-activated cell sorting (FACS). The transfected cell pellets were resuspended in primary antibody solution (mouse anti-Rhodopsin), and incubated on ice for 1 h. After centrifuging for 3 min at 200 × *g* and aspirating all solution, the cell pellets were resuspended in secondary antibody solution (Phycoerythrin-conjucated anti-mouse IgG), and incubated for 30 min on ice. At the end of the

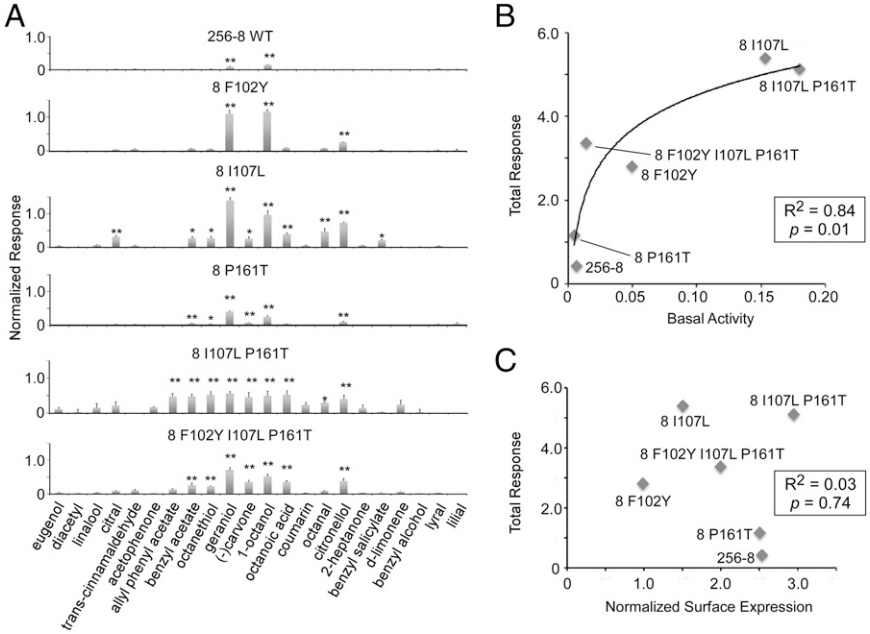

Fig. 5. Mutations at a single or a few residues are sufficient to convert MOR256-8 to broadly responsive ORs. (*A*) Responses of different ORs to a set of 22 odorants after subtracting the basal activity. All odorants were tested at 300 μM and the data for each OR were averaged from three repeats on the same plate (mean ± SEM). All odorant responses and basal activities were normalized to WT MOR256-3's response to 1-octanol at 300 μM and corrected for surface expression. A positive response was identified if it was significantly higher than the basal activity (*$P < 0.05$ and **$P < 0.01$ in one-way ANOVA post hoc Dunnett's tests). (*B*) The total response (sum of the responses to all 22 odorants at 300 μM) was plotted against its basal activity for each OR. All activities were normalized to WT MOR256-3's response to 1-octanol at 300 μM and corrected for surface expression. The curved line represents logarithmic regression fitting. (*C*) The total response was not correlated with the receptor surface expression (linear regression analysis). The surface expression of each OR was normalized to that of WT MOR256-3.

incubation, the cells were centrifuged, and the cell pellets were suspended with washing solution in 5-mL round-bottomed tubes (BD Falcon). Cells were analyzed using a FACS machine (Flow Cytometry and Cell Sorting Resource Laboratory, University of Pennsylvania) according to the GFP and PE fluorescent signals. The fluorescent range of the GFP and PE were determined by control cells transfected with GFP or receptor plasmid only. Cells transfected with GFP only were also used to determine the nonspecific PE fluorescence.

Three-Dimensional Atomic Models. The protocol follows a published method (27). Sequences of MOR256-3, 256–8, 256–17, 256–22, 256–31, ml7 (olfr2), mOR-EG (olfr73), and S25 (olfr480) are aligned with 396 human ORs (28) and nine sequences of X-ray elucidated GPCRs: bovine rhodopsin [Protein Data Bank (PDB) ID 1U19] (29), human beta 2 adrenergic (PDB: 2RH1) (30), turkey beta 1 adrenergic (PDB ID 2VT4) (31), human chemokine receptors CXCR4 (PDB ID 3ODU) (32) and CXCR1 (PDB ID 2LNL) (33), human dopamine receptor D3 (PDB ID 3PBL) (34), human adenosine a2A receptor (PDB ID 2YDV) (35), human histamine H1 receptor (PDB ID 3RZE) (36), and muscarinic acetylcholine receptor M2 (PDB ID 3UON) (37). Highly conserved motifs in ORs were considered as constraints for the alignment: GN in helix 1, PMYFFLXXLSXXD in helix 2, MAYDRYXAICXPLXY in helix 3, SYXXI in helix 5, KAFSTCASH in helix 6, LNPXIY in helix 7 and a pair of conserved cysteines $97^{3.25}$-179^{EC2}, which constitute a known disulfide bridge between the beginning of helix 3 and the extracellular loop 2. Four experimental GPCR structures (1U19, 3ODU, 2YDV, and 2LNL) were selected as templates to build MOR256-3 by homology modeling with Modeler (38). The N-terminal structure (residues 1–18) was excluded to avoid perturbation of the modeling protocol with a nonstructured part of the protein.

ACKNOWLEDGMENTS. We thank Dr. Yun R. Li for her contributions at the early stage of this project and Dr. Joel Mainland for critical reading of the manuscript. This work was supported by grants from the National Institute on Deafness and Other Communication Disorders, National Institute of Health Grants DC011554 and DC006213 (to M.M.) and DC005782 and DC012095 (to H.M.), National Science Foundation (NSF) Grants 1515801 and 1515930 (to H.M. and M.M.) and Neurolf project Agence Nationale de la Recheche (ANR) (to J.G.) as part of NSF/NIH/ANR Collaborative Research in Computational Neuroscience, and Appel à Project Exploratoire (APEX) Région Provence-Alpes-Côte d'Azur (PACA) (Olfactome project to J.G.).

1. Buck L, Axel R (1991) A novel multigene family may encode odorant receptors: A molecular basis for odor recognition. *Cell* 65(1):175–187.
2. Touhara K, Vosshall LB (2009) Sensing odorants and pheromones with chemosensory receptors. *Annu Rev Physiol* 71:307–332.
3. Grosmaitre X, et al. (2009) SR1, a mouse odorant receptor with an unusually broad response profile. *J Neurosci* 29(46):14545–14552.
4. Nara K, Saraiva LR, Ye X, Buck LB (2011) A large-scale analysis of odor coding in the olfactory epithelium. *J Neurosci* 31(25):9179–9191.
5. Saito H, Chi Q, Zhuang H, Matsunami H, Mainland JD (2009) Odor coding by a Mammalian receptor repertoire. *Sci Signal* 2(60):ra9.
6. Li J, Haddad R, Chen S, Santos V, Luetje CW (2012) A broadly tuned mouse odorant receptor that detects nitrotoluenes. *J Neurochem* 121(6):881–890.
7. Kobilka B (2013) The structural basis of G-protein-coupled receptor signaling (Nobel Lecture). *Angew Chem Int Ed Engl* 52(25):6380–6388.
8. Lefkowitz RJ (2013) A brief history of G-protein coupled receptors (Nobel Lecture). *Angew Chem Int Ed Engl* 52(25):6366–6378.
9. Dror RO, et al. (2011) Activation mechanism of the β2-adrenergic receptor. *Proc Natl Acad Sci USA* 108(46):18684–18689.
10. Vaidehi N, et al. (2002) Prediction of structure and function of G protein-coupled receptors. *Proc Natl Acad Sci USA* 99(20):12622–12627.
11. Kohlhoff KJ, et al. (2014) Cloud-based simulations on Google Exacycle reveal ligand modulation of GPCR activation pathways. *Nat Chem* 6(1):15–21.
12. Abaffy T, Malhotra A, Luetje CW (2007) The molecular basis for ligand specificity in a mouse olfactory receptor: A network of functionally important residues. *J Biol Chem* 282(2):1216–1224.
13. Lai PC, Singer MS, Crasto CJ (2005) Structural activation pathways from dynamic olfactory receptor-odorant interactions. *Chem Senses* 30(9):781–792.
14. Charlier L, et al. (2012) How broadly tuned olfactory receptors equally recognize their agonists. Human OR1G1 as a test case. *Cell Mol Life Sci* 69(24):4205–4213.
15. de March CA, Golebiowski J (2014) A computational microscope focused on the sense of smell. *Biochimie* 107(Pt A):3–10.
16. Katada S, Hirokawa T, Oka Y, Suwa M, Touhara K (2005) Structural basis for a broad but selective ligand spectrum of a mouse olfactory receptor: Mapping the odorant-binding site. *J Neurosci* 25(7):1806–1815.
17. Gelis L, Wolf S, Hatt H, Neuhaus EM, Gerwert K (2012) Prediction of a ligand-binding niche within a human olfactory receptor by combining site-directed mutagenesis with dynamic homology modeling. *Angew Chem Int Ed Engl* 51(5):1274–1278.
18. de March CA, et al. (2015) Conserved residues control Activation of mammalian G protein-coupled odorant receptors. *J Am Chem Soc* 137(26):8611–8616.
19. Haddad R, et al. (2008) A metric for odorant comparison. *Nat Methods* 5(5):425–429.
20. de March CA, et al. (2015) G protein-coupled odorant receptors: From sequence to structure. *Protein Sci* 24(9):1543–1548.
21. Venkatakrishnan AJ, et al. (2013) Molecular signatures of G-protein-coupled receptors. *Nature* 494(7436):185–194.
22. Goddard WA, 3rd, Abrol R (2007) 3-Dimensional structures of G protein-coupled receptors and binding sites of agonists and antagonists. *J Nutr* 137(6, Suppl 1): 1528S–1538S, discussion 1548S.
23. Baud O, et al. (2011) The mouse eugenol odorant receptor: Structural and functional plasticity of a broadly tuned odorant binding pocket. *Biochemistry* 50(5):843–853.
24. Hallem EA, Carlson JR (2006) Coding of odors by a receptor repertoire. *Cell* 125(1):143–160.
25. Tian H, Ma M (2004) Molecular organization of the olfactory septal organ. *J Neurosci* 24(38):8383–8390.
26. Zhuang H, Matsunami H (2008) Evaluating cell-surface expression and measuring activation of mammalian odorant receptors in heterologous cells. *Nat Protoc* 3(9):1402–1413.
27. Charlier L, et al. (2013) Molecular modelling of odorant/olfactory receptor complexes. *Methods Mol Biol* 1003:53–65.
28. Zozulya S, Echeverri F, Nguyen T (2001) The human olfactory receptor repertoire. *Genome biology* 2(6):RESEARCH0018.
29. Okada T, et al. (2004) The retinal conformation and its environment in rhodopsin in light of a new 2.2 A crystal structure. *J Mol Biol* 342(2):571–583.
30. Cherezov V, et al. (2007) High-resolution crystal structure of an engineered human beta2-adrenergic G protein-coupled receptor. *Science* 318(5854):1258–1265.
31. Warne T, et al. (2008) Structure of a beta1-adrenergic G-protein-coupled receptor. *Nature* 454(7203):486–491.
32. Wu B, et al. (2010) Structures of the CXCR4 chemokine GPCR with small-molecule and cyclic peptide antagonists. *Science* 330(6007):1066–1071.
33. Park SH, et al. (2012) Structure of the chemokine receptor CXCR1 in phospholipid bilayers. *Nature* 491(7426):779–783.
34. Chien EY, et al. (2010) Structure of the human dopamine D3 receptor in complex with a D2/D3 selective antagonist. *Science* 330(6007):1091–1095.
35. Lebon G, et al. (2011) Agonist-bound adenosine A2A receptor structures reveal common features of GPCR activation. *Nature* 474(7352):521–525.
36. Shimamura T, et al. (2011) Structure of the human histamine H1 receptor complex with doxepin. *Nature* 475(7354):65–70.
37. Haga K, et al. (2012) Structure of the human M2 muscarinic acetylcholine receptor bound to an antagonist. *Nature* 482(7386):547–551.
38. Eswar N, et al. (2006) Comparative protein structure modeling using Modeller. *Curr Protocols Bioinformatics* Chapter 5:Unit 5 6.